Tribological Behavior of Plasma Sprayed Al_2O_3 and ZrO_2 5CaO Coatings on Al-6061 Substrate

N. Krishnamurthy[1*], M.S.Murali[2] and P.G.Mukunda[3]

[1,3]*Nitte Meenakshi Institute of Technology, Bangalore, India*
[2]*Auden Technology and Management Academy, Bangalore, India*

(Received January 6, 2010: final form March 5,2010)

ABSTRACT

Plasma spraying is one of the methods used for combating wear. The processing of materials using plasma spraying leads to inhomogenities, such as un-melted particles, oxide particles, oxide inclusions and porosity and the structure markedly different from that of cast, wrought or even powder metallurgy materials. Despite of its wide spread industrial use, little is known about the basic friction behavior and mechanism by which such coatings wear. In this work, the abrasive wear resistance of plasma sprayed Al_2O_3 and ZrO_25CaO coatings has been investigated through pin-on-disc test according to ASTM G99. From the investigation it was found that the wear rate is mainly affected by load applied, splats, porosity and microhardness of coatings. The coefficient of friction was found to be more significantly effected by load than other test parameters. This study showed that pin on disk is a well controlled test and can be used to understand certain basic relationships between the sliding friction and wear behavior of plasma sprayed coatings. It also includes the characterization of coating systems.

Keywords: Plasma spraying, Thermal barrier coatings, Microstructure, Wear, Coefficient of Friction

*Corresponding Author's E-Mail:
krishamu@rediffmail.com

1. INTRODUCTION

Due to market pressures for improvements in productivity, reliability, durability, wear resistance as well as the profitability of mechanical systems, manufacturers are placing increasing demands on available materials. Economic constraints require that these materials are inexpensive and easily available. In order to enhance the surface properties of today's materials, producers of components are turning to different surface treatments and in particular to hard protective coatings /1/. Thermal Barrier Coatings (TBCs) have been used extensively as one of the hard protective coating for so many engineering components /2-7/. TBCs are used to improve fuel efficiency by insulating the combustion chamber components of engine, there by recovering 8 to 15% of the energy that is attributed to heat losses. These coatings have been applied to the cylinder head, the valves, the piston and liner, etc.

Thermal Barrier and wear resistant coatings are produced using Thermal spraying method which is often considered as a potential alternative to traditional coating manufacturing techniques such as hard chrome electroplating, Physical Vapor Deposition (PVD), Chemical Vapor Deposition (CVD), etc. /8-10/. Among various thermal spraying techniques, plasma spraying has been widely employed to provide an improved wear resistance to various industrial parts /11-15/. The plasma

sprayed ceramic coatings possess very high hardness. Due to their purely ceramic nature, they are almost insensitive to many corrosive environments and can withstand high temperatures /16/. These coatings are made up of layers that are formed when melted material droplets flatten and solidify on the surface of the substrate /17/. Because of their lamellar structure, the coatings have various amounts of force. This variable force and incomplete bonding between lamellae decrease the strength, wear resistance and the corrosion resistance of the coatings. The variety of defects present in plasma sprayed coatings make the modeling of wear properties difficult. However it has been shown that coatings with more homogeneous and denser structure perform better than badly structured coating in abrasion. Inhomogeneities tend to cause local fractures. The coupling between hardness and wear resistance is often unclear, presumably because of the low fracture toughness /18, 19/.The wear behavior of plasma sprayed Al_2O_3 coatings conducted in a block-on ring tester, was reported to be dominated by plastic deformation and adhesive wear as well as brittle fracture /20/.

Zirconia based ceramic coatings have been used in engines and gas turbines as thermal barrier coatings. Plasma spraying of these materials could enhance the thermal efficiency /21-26/ of internal combustion engines and increase the service life of piston ring or cylinder liner pairs. Zirconia as coating is interesting materials because of its outstanding mechanical, thermal, optical and electrical properties. It has high melting point, high resistance to oxidation, low thermal conductivity and high co-efficient of thermal expansion.

A thorough study of the wear resistance of thermally sprayed coatings must involve plasma sprayed ceramics, which could represent an economical alternative to High Velocity Oxygen Fuel (HVOF) sprayed cermets in some industrial applications. Much research related to the basic wear mechanisms of plasma sprayed oxides exists, since such coatings have been studied for a long time /27-30/. However, there exists an ambiguity in understanding the basic mechanisms of wear whether is it by adhesion or abrasion.

The main objective of this investigation is to obtain experimental data on the wear rates, wear mechanisms, coefficient of friction of various plasma sprayed coatings under different load conditions and dry environment.

2. EXPERIMENTAL DETAILS

2.1 Plasma spraying:

Circular pins of diameter 12 mm and length 25 mm and plates of 100mm x 100mm x 5mm thick made of Al-6061 were selected as substrates to prepare coated samples for wear testing and surface texture measurements respectively. The composition of Al-6061substrate is given in **Table 1**.

Table 1
Chemical composition of substrate and coating materials

Substrate material			
Al-6061			
Si-0.65, Fe-0.25, Cu-.25, Mn-0.3, Mg-0.89, Zn-0.1, Cr-0.07, V-0.01, Ti-0.82, Al-balance			
Coating material			
Metco105SFP (TC1)	Metco 201NS (TC2)	Metco 446 (BC1)	Metco 410NS (BC2)
99.5 Al_2O_3	ZrO_2 5CaO	Al 25Fe7Cr5Ni	$Al_2O_3$30(Ni 20Al)

TC1-Top Coat 1, TC2-Top Coat 2, BC1-Bond Coat 1, BC2-Bond Coat 2

The dimensions and surface finish of the substrates were checked. Then substrates were degreased by immersing in a vapor bath of tetra chloro-ethylene boiled at 343 to 353 K (70 to 80 ^{o}C). The surfaces to be coated were grit blasted using Al_2O_3 grains (-18+24 mesh) with a pressure of 455kPa. The coating process was accomplished with a Sulzer Metco plasma spraying equipment. The trade name and chemical composition

of bond and top coat powders are given in Table1. The spray parameters for different materials are shown in **Table 2.** The schematic diagrams of coating layers on Al-6061 substrate are shown in **Figure 1.**

Table 2
Plasma spray parameters for different coating materials used

Materials	Primary gas (Argon) pressure kPa	Secondary gas(H_2) Pressure kPa	Carrier gas (Argon) Flow lpm	Current A	Voltage V	Spray distance mm	Feed rate Kg/hr
TC1	700	520	60	600	65	64-125	2.7
TC2	345	345	37	500	75	50-100	5.4
BC1	520	340	37	500	70	100-150	3.2
BC2	700	340	37	500	65	100-175	4.1

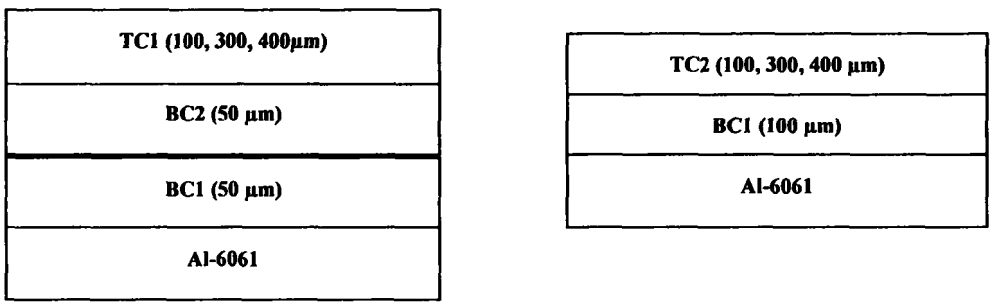

Al-S1, Al-S2 and Al-S3 Al-S4, Al-S5 and Al-S6

Fig 1: Schematic diagrams of coating layers with Al-6061 substrate (number in the bracket indicates the actual thickness of each layer)

2.2 Measurement of surface texture parameters

For surface texture measurement, coated plates of 100mmx100mm were divided into small rectangles of 10mmx10mm dimensions. For each rectangle the average roughness was measured using Mahr Perthometer. A 3D profile was drawn for each coated specimen taking average roughness in vertical coordinate. Coating microstructure (morphology and cross section) was studied using JOEL-JAPAN JSM-840A Scanning Electron Microscope.

The porosity of each coating system was measured using an Image Analyzer.

2.3 Tribological testing

Friction and wear tests were carried out on coated specimens using DUCOM Pin-on Disk tribometer. A 60 grit Al_2O_3 abrasive wheel was used as disk. The specification of the wheel is given as WA60K5V. Three series of tests were performed on each coating system with normal loads of 5, 10 and 15 N, track diameter of 80mm and a speed of 200rpm under atmospheric conditions. The sliding distance was kept constant at 378m. Wear rate and friction coefficient were recorded. The tribometer used for wear testing is shown in **Figures 2** and **3.**

3. RESULTS AND DISCUSSION

3.1 Coating mechanism

Al_2O_3 coated test samples viz., Al-S1, Al-S2 and Al-S3 are characterized by their disc shaped grains

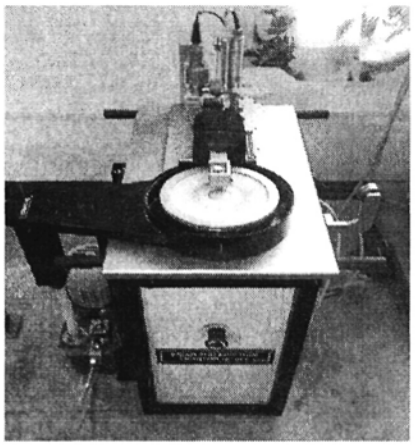

Fig. 2: Tribometer

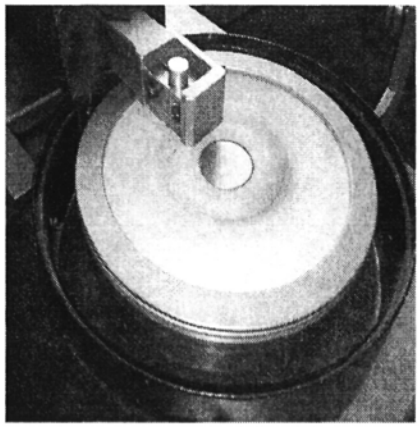

Fig. 3: Pin on Disk

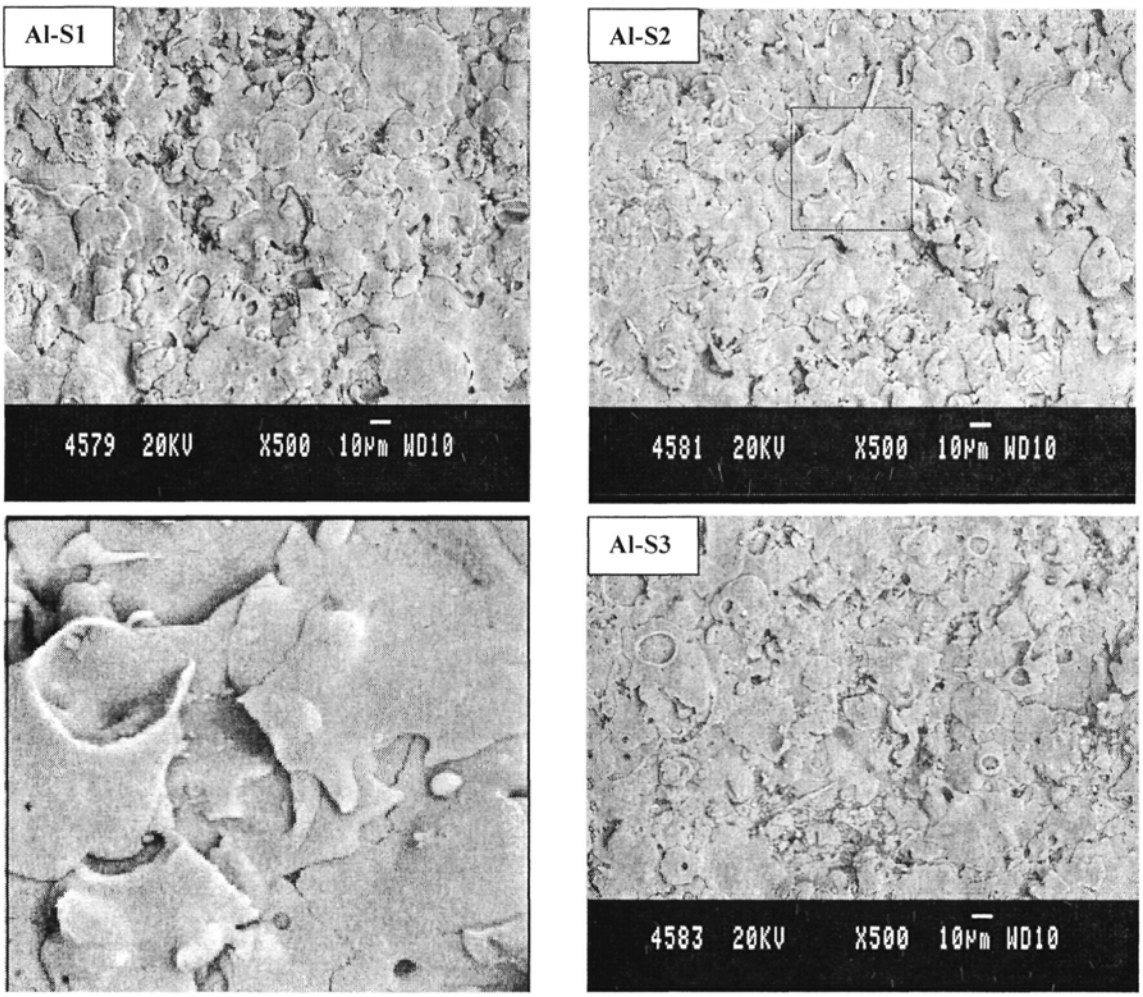

Enlarged view of the region marked in Al-S2 showing micro-cracks

Fig. 4: Morphology of Al_2O_3 Coatings

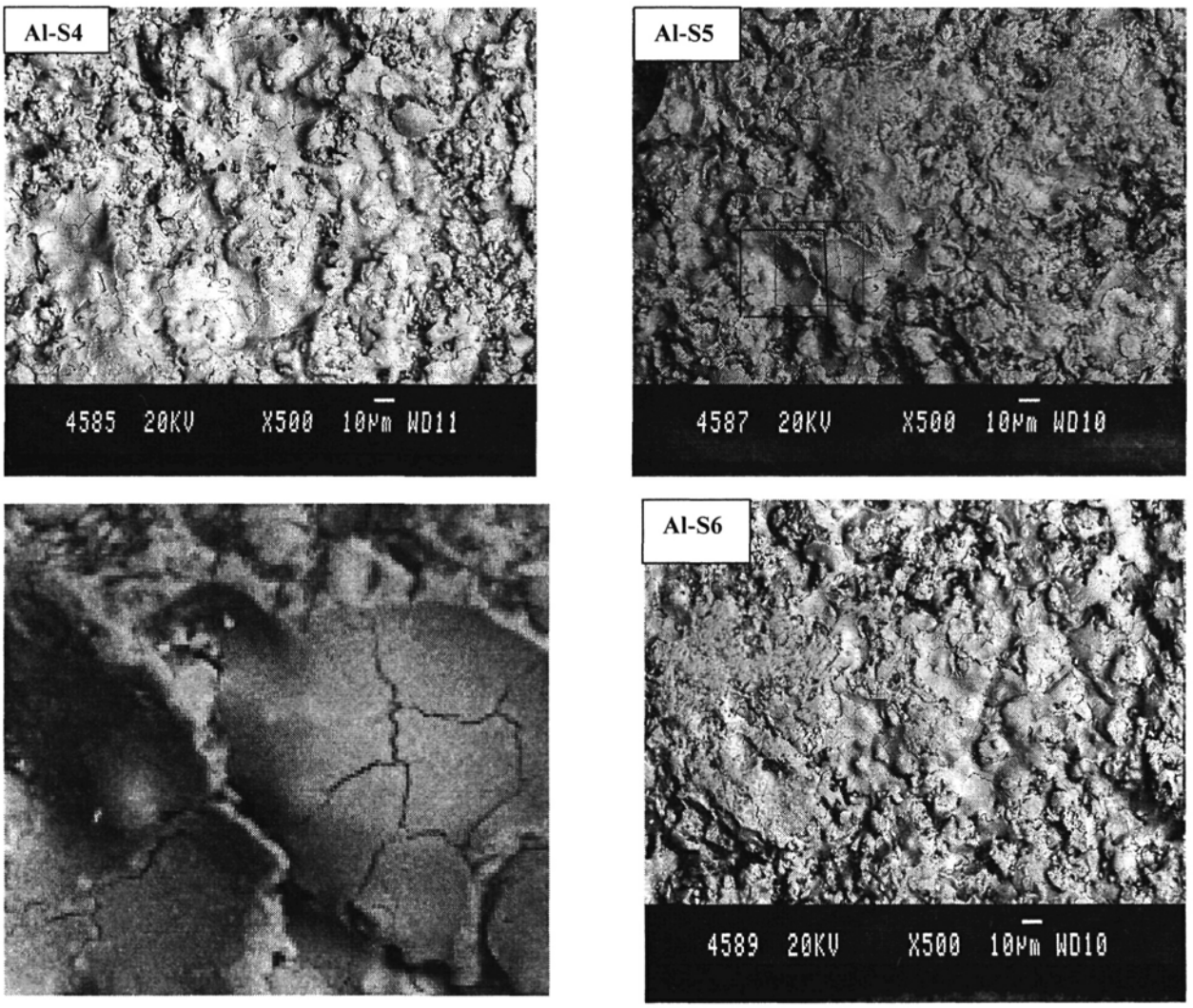

Enlarged view of the region marked in Al-S5 showing micro-cracks

Fig. 5: Morphology of $ZrO_2$5CaO Coatings

(**Figures 4** and **5**). These grains are found to be the flattened solidified droplets of the coating material. The molten particles are found to be distributed more or less evenly producing a smooth coating surface. Enlarged view of marked region of Al-S2 sample (**Figure 4**) indicates a network of microcracks. Cracks are also observed on the surface of flattened droplets. This may possibly be due to the presence of residual stresses introduced by thermal shocks resulted during the spraying process. Increasing the thickness of top coat appears to have no significance on the microstructure as in the case with test samples Al-S2 and Al-S3 (**Figure 4**).

$ZrO_2$5CaO coated test samples such as Al-S4, Al-S5 and Al-S6 exhibit a dense undulated structure (**Figure 5**). The enlarged view of marked region of Al-S5 sample indicates a network of microcracks. The sizes of these microcracks appear to be slightly larger than that observed of Al_2O_3 coated test samples. It is possibly due to the large difference in the magnitude of thermal conductivity between the substrate and coated material. The thermal conductivity of $ZrO_2$5CaO is found to be between 2 to 4 $Wm^{-1}K^{-1}$, where as it varies from 160 to 170 $Wm^{-1}K^{-1}$ for Al-6061. Heat is generated during the spraying process which in turn can contribute to the presence of cracks. On the other the thermal

conductivity of alumina varies between 33 to 37 $Wm^{-1}K^{-1}$, thus difference in the thermal conductivity with the substrate is much less in comparison with the previous case coating to lower thermal stresses encountered in the case of Al_2O_3 coated test samples. Further, the splats in the coatings are separated by inter-lamellar pores resulting from rapid solidification of the lamellae and very fine voids are being formed due to incomplete inter-splat contact in and around un-melted particles.

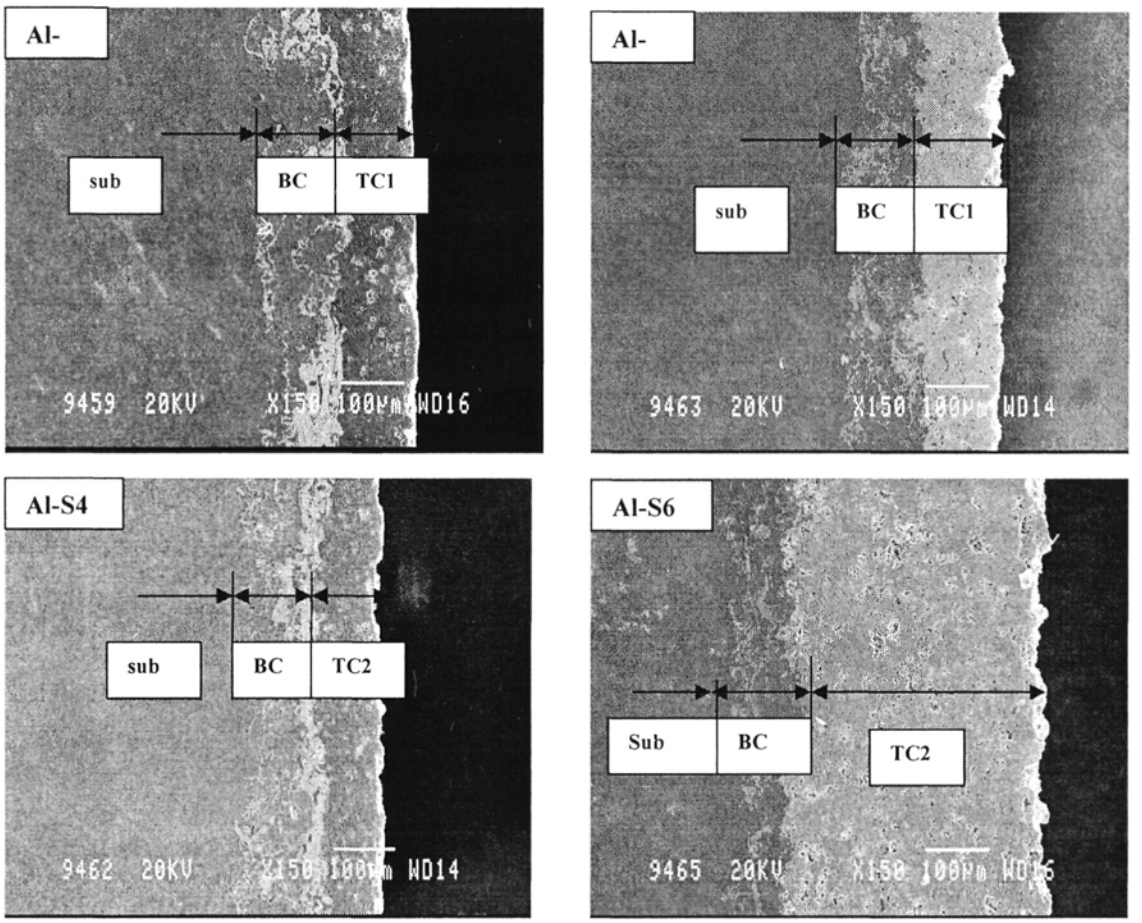

Fig. 6: Scanning electron micrographs, showing cross-section of Al-S1, Al-S3, Al-S4 and Al-S6 samples (sub-substrate, BC-bond coat, TC1-top coat 1, TC2-top coat 2)

Table 3
Thicknesses, Porosity and Average Surface Roughness of Coatings

Coating System	Average Thickness (μm)		Average Porosity (%)			Avg. Surface Roughness (μm)		
	BC1+BC2	TC1/TC2	BC1	BC2	TC1/TC2	BC1	BC2	TC1/TC2
Al-S1	95	104	5.5	5.9	6.4	3.6	5.5	4.42
Al-S2	86	260	5.8	6.2	6.7	3.8	5.3	5.4
Al-S3	102	365	6.2	6.7	7.0	3.8	5.65	5.85
Al-S4	100	95	6.8	----	8.5	3.9	----	6.3
Al-S5	105	270	7	----	8.9	4.0	----	6.6
Al-S6	85	390	7.1	----	9.2	3.9	----	6.8

3.2 Coating Thicknesses and Porosity

Thicknesses of Al_2O_3 and ZrO_25CaO coatings measured along the cross section of the samples (**Figure 6**) are shown in **Table 3**. It is observed that the variation in coating thickness is between ±15μm to ±30μm from the actual required thickness. This is attributable to the variations in speed of the gun during plasma spraying process. This variation can be eliminated by applying Robot Plasma spraying. Sample polishing technique is also found to influence the accuracy of measurements of the thickness of the coating.

The porosity in Al_2O_3 coating systems is in the range of 5.5 to 6.4% in case of bond coat and it varies between 6.4 to 7.1% in case of top coat. The porosity in ZrO_25CaO coating systems varies between 6.3 and 6.8% in case of bond coat and 8.2 to 9.4% in case of top coat. Porosity is high, due to formation of rounded pores which are produced by unmelted particles, splats, stacking faults and gas entrapment. Porosity of coatings is found to increase with increase in the thickness of top coat.

3.3 Surface Texture of Coatings

Average roughness of different coatings is indicated in **Table 3.**

It is evident that the average roughness values of alumina coatings vary between 3.5 and 5.5 μm while it is between 4.5 and 7.2 μm in case of ZrO_25CaO coatings. Top coat of test samples such as Al-S4, Al-S5, Al-S6 possess mounds of molten and unmolten particles which contribute to the increase in roughness. Flowability of ZrO_25CaO is less compared to that of alumina and this contributes to the formation of mounds and affects the quality of the surface texture of the coating. Increase in porosity as well as the coating thickness enhances the roughness of top coat. Similar observations regarding to the effect of coating thickness on roughness were reported by Sarikaya /31/.

Figure 7 shows the roughness profile of some of the coating systems with average roughness (Ra) as the main parameter.

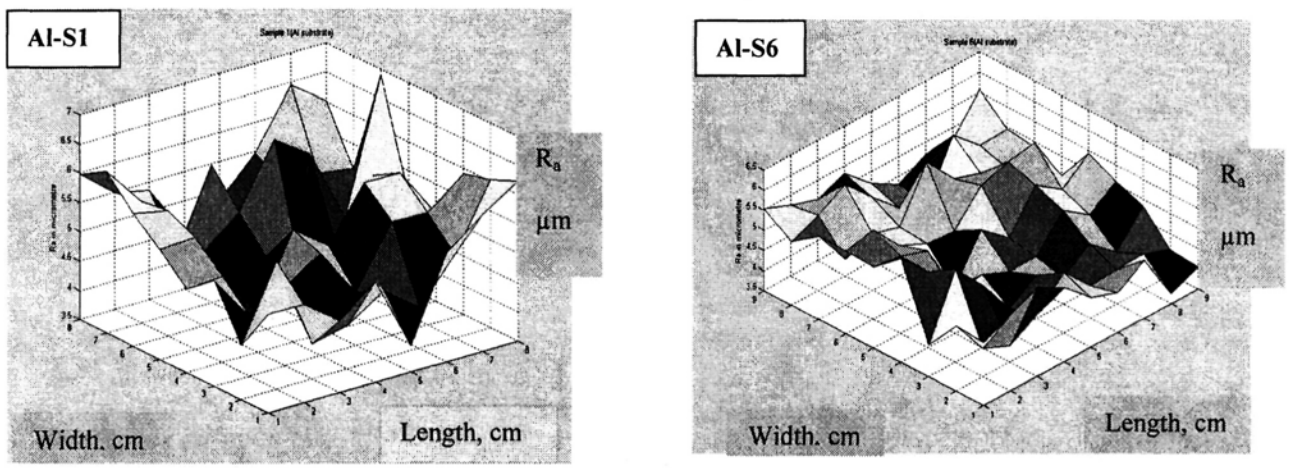

Fig. 7: 3D surface profile of Al-S1 and Al-S6 coating systems

3.4 Microhardness of Coatings

Hardnesses of different layers of coating systems are indicated in **Table 4.** It is evident that there is a marked difference in microhardness of different layers of coatings. For the samples of Al-6061 substrate, substrate hardness varies from 80 to 88 HV, whereas the hardness of BC1, BC2 and TC1 in case of Al-S1, Al-S2 and Al-S3 samples varies from 120 to 130 HV, 140 to 148 HV and 1100 to 1180 HV respectively. In case of Al-S4, Al-S5, Al-S6 samples, the hardness of BC1 and TC2 varies from 119 to 120 HV and 800 to 850 HV respectively. It is also observed that for the first three Al

series coating systems, the BC1 thickness is about 50μm and for the next three coatings it is about 100 μm. From this data it can be realized that the microhardness of BC1 decreases as its thickness increases. Similarly, the hardness of TC1 and TC2 decreases with the increase in their thicknesses. Further, the hardness of Al_2O_3 coatings is found to be more than that of ZrO_25CaO coatings. It is also evident that the micro hardness measurements exhibit a wide dispersion. Such dispersion in the microhardness values of the coatings is a typical characteristic of APS ceramic coatings clearly attributable to their microstructural heterogeneity /32/.

Table 4
Hardness of Coating Systems

Samples	Hardness $HV_{0.3}$			
	Substrate	BC1	BC2	TC1/TC2
Al-S1	86	120	140	1180
Al-S2	84	127	145	1140
Al-S3	88	130	148	1100
Al-S4	88	120	----	850
Al-S5	84	119	----	830
Al-S6	80	120	----	800

3.5 Coefficient of Friction and Wear Rates

Load or contact stress is the most relevant and easily monitored parameter which can influence wear. The magnitude of the normal load or the contact stress is important since it increases both the area of contact and depth below the surface at which the maximum shear stress occurs as well as influencing the elastic or plastic deformation state. Variation of Coefficient of Friction (COF) against 5, 10 and 15 N loads under dry sliding conditions for coating systems are shown in **Figure 8**. It is observed that all the coating systems investigated here under 5, 10 and 15 N loads exhibit of three stages in the variation of COF. The first stage consists of a very short period of an increase in COF related to a start up step. Second stage shows a small decrease in COF and after the decrease, the COF almost remains constant for some period. Third stage consists of a small increase in COF till the end of cycle. The causes for these three stages can be explained as follows. At the beginning of testing, the increase in COF is prominent due to the initial roughness of the two contacting surfaces. From the SEM micrographs of as-sprayed coatings (**Figures** 4 and 5), it is seen that the top coat possesses semi molten (partly melted) and un-molten (unmelted) splats. Wear debris is generated from these particles during the running-in-period. Thus, the process of wear after the initial running-in-stage translates to the three body abrasion situation rather than two body sliding with the release of wear debris. This appears to be the main reason for the rise in COF during this running-in-period. The increase in coefficient of friction during running-in-period is also reported by earlier investigators /33/. The increase in COF may also be due to the removal of hard reinforcement from the comparatively soft matrix of the coating. The ploughing action during this period is likely to cause an increase in tangential forces, which in turn contributes to the increase in coefficient of friction. The decrease in coefficient of friction in the second stage is due to the smoothening of top coat hard particles that were not removed during the first stage. This process produces a glazed surface in the coating. From this step onwards, the COF remains more or less same until the top coat is removed. In the third stage, it is anticipated that bond coat of the specimen comes in contact with the disk. Since the bond coat material is soft compared to top coat, material removal will be rapid which inturn increases the coefficient of friction. The SEM micrographs of worn surfaces (**Figure 9**) of coating systems on Al-6061 substrate shows that about 60 to 70% area of top coat is removed exposing the bond coat under 5 N load. This is found to increase with the increase in load at 10 and 15 N. From this observation, it can be realized that the increase in COF is mainly due to exposition of bond coat to counter body (abrasive disk) surface.

3.6 Effect of Load, Porosity and Surface Roughness on Coefficient of Friction

It is observed that coefficient of friction increases with the increase in load (**Figure 8**). It is mainly due to the increase in contact area between the coated pin and the abrasive disk. It is also seen that in many cases coefficient of friction is found to increase with the increase in the thickness of top coat. It is mainly due to increase in porosity and roughness of coating with respect to thickness of coating /31/. From the graphs, it

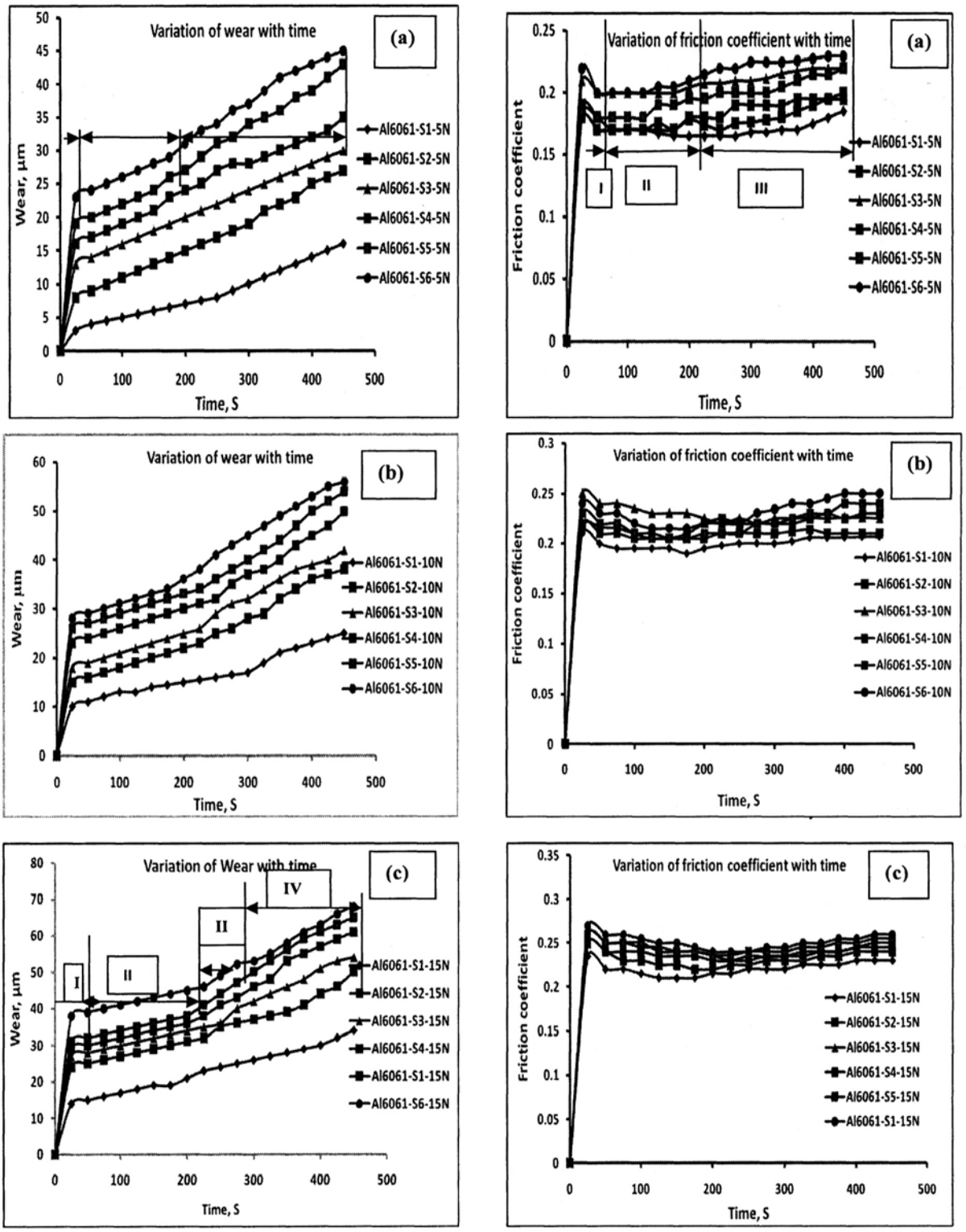

Fig. 8: Variation of Wear Loss and Coefficient of Friction under Different Load Conditions for Coatings on Al-6061 Substrate (a) 5 N Load (b) 10 N Load (c) 15 N Load

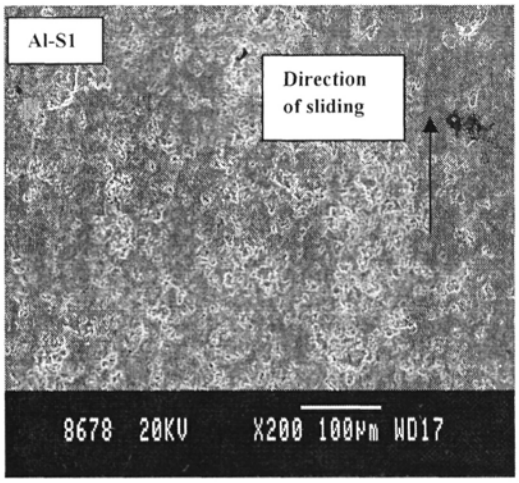

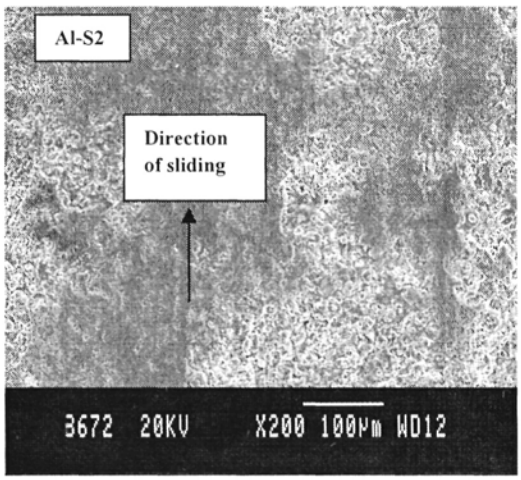

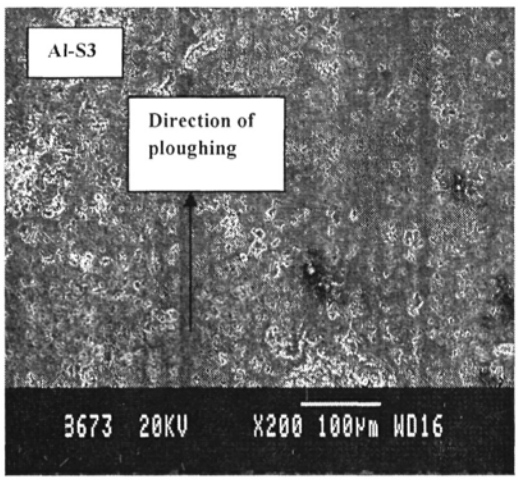

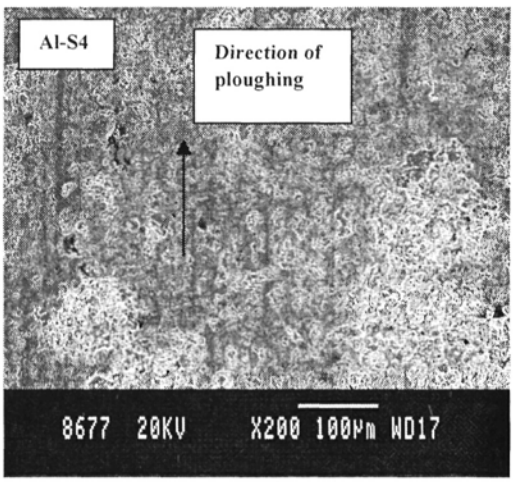

(a)

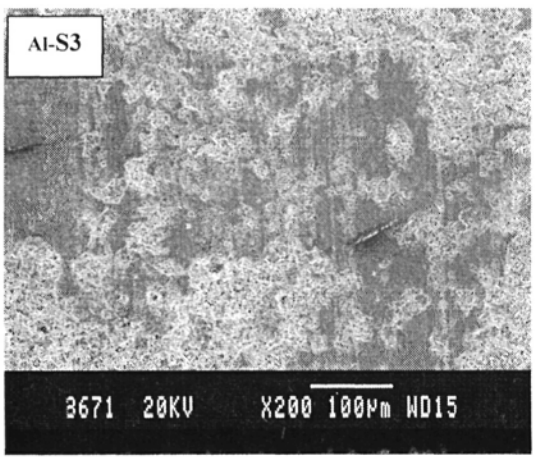

(b)

Continued ...

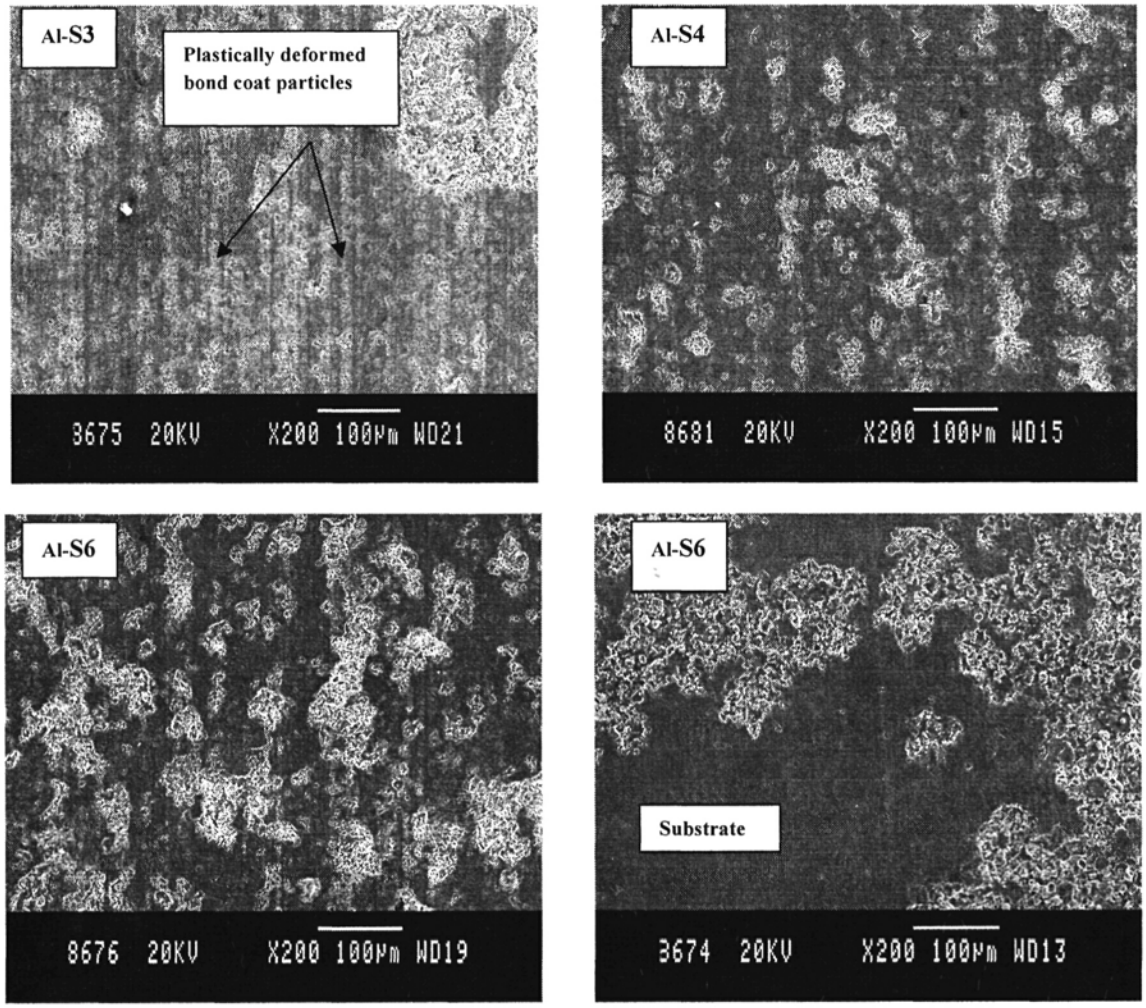

(c)

Fig. 9: SEM Micrographs of Worn Surfaces of Coatings Systems on Al-6061 Substrate under (a) 5 N Load (b) 10 N Load (c) 15 N Load

is also observed that the coefficient of friction is high for $ZrO_2$5CaO coatings since the roughness of these coatings is also higher compared to that of Al_2O_3 coatings.

3.7 Wear of Coating Systems

Wear loss graphs of coatings under 5 and 10 N loads (**Figure 8**) show three distinct stages. The first stage consists of sudden increase in amount of wear for a short period of time due to abrasion between the asperities of top coat and the abrasive disk. The second stage comprises of slightly increase in wear for some period due to top coat abrading. The third stage exhibits a further increase in wear which is due to exposure of bond coat to abrasive disk. Further in the case of coating systems subjected to 15 N loads, one more stage is apparent due to the rubbing of substrate with abrasive disk

3.8 Wear Mechanism

Microscopic observation of the worn surfaces of coatings (**Figure 9**) indicates that the wear of top coat which is mainly a ceramic layer takes place by ploughing mechanism. This wear mechanism is also referred to as exfoliation mechanism of wear /32/. According to this mechanism, friction would result in

the initiation of crack between two splats of the same lamella. During cyclic loading, the crack is found to have been propagating along the splat boundary, leading to its final exfoliation from the worn surface. The stress field developed during sliding also led to the initiation of cracks perpendicular to the coating/substrate interface and they are found to propagate through the thickness of the coating. In case of Atmospheric Plasma Sprayed Al_2O_3 or ZrO_25CaO coatings, the weak interfaces between the successive lamellae appears to have been failed, leading to the delamination of the coating which is extended from the axis of loading. This degradation mechanism appears to be contributing to the rapid wear of the ceramic coating and hence an increase in the wear.

The mechanism of wear in case of bond coat is similar to that of adhesive wear. The surface tribofilm formation is an important tribological phenomenon in this type of mechanism. These tribofilms consist of plastically deformed wear debris, plastically deformed coating material or chemically altered coating surfaces /34/. In the absence of tribofilm formation, the coating would not oppose the continuous material removal by the harder counterpart asperities. The tribofilm formation, however, is only beneficial if it possesses adequate cohesion. In the present investigation, there is a possibility for the formation of tribofilm between counterpart and bond surface due to release of wear debris. During the wear test, the debris formed due to wear of the coating is continuously being wiped off with a brush. It prevents the formation of tribofilm leading to increase in wear in this stage. Micrographs of worn surfaces of some of the coatings under 10 N and 15 N loads show plastically deformed bond coat particles substantiating the fact that wear has mainly taken place because of adhesion. The adhesion wear behaviour can also be seen when the substrate is exposed to abrasive disk. Al6061 substrate which is very soft undergoes severe wear by the embedding of wear debris into the hard particles of abrasive disk. The increase in wear loss occurs till the embedding process of the particles to the disk becomes saturated. The wear then starts decreasing. This is mainly due to the glazed property of embedded layer of the disk. Therefore it is suggested that this embedded layer has to be removed periodically to obtain a quantifiable relationship between wear loss and time.

Micrographs of worn surfaces (**Figure 9**) indicate that the width of the wear track increases with the increase in load. This is attributable to the increase in the initial contact area of the coating with abrasive disk. Plough marks are observable on the wear tracks of top coat. From the micrographs, it is found that the wear tracks of bond coat and substrate consist of plastically deformed material. The 15 N load wear track appears to have deeper plough marks in comparison to those tracks on which wear tests are carried out at 5 and 10 N loads. This is mainly due to the fact that trapping of particles between the harder disk and soft coating under the highest load which would indent deeper into the coating, more prominent plough marks, and hence leading to greater amount of material removal.

3.9 Effect of Grain Size and Microstructure on Wear

In certain cases one or more factors will dominate wear resistance of the material. The microstructure of ceramics, especially its grain size has an immense influence on its wear resistance. The coating which has a finer grain size experience higher wear loss. It is observed that the grain size of ZrO_25CaO (-53+11μm) powder is more than that of Al_2O_3 (-31+3.9μm) powder. As discussed earlier, ZrO_25CaO coating systems have experienced significantly higher wear loss in comparison with those samples having Al_2O_3 coatings, clearly demonstrating meaningful relationship between the grain size of powder and the wear loss of coatings. The increase in grain size is found to increase the surface roughness and porosity of the coatings which inturn contributes to enhanced wear loss.

The changes in microstructure are significant in case of wear resistance of plasma sprayed coatings. It is found that the phase transformation has an important effect on the wear process. There is a preferential growth in the changes due to the process of powders and additives. This preferential growth certainly affects the wear behaviour of coatings to some degree. It is safe to say that different microstructures of coatings make different contribution to the wear resistance. Phase analysis of Al_2O_3 coatings show that an incomplete transformation of Al_2O_3 into γ-Al_2O_3 has occurred

during plasma spraying process. The presence of α-Al_2O_3 in coatings can resist the wear loss. This is also one of the possibilities in case of Al_2O_3 coatings not exhibiting higher wear in comparison with ZrO_25CaO coatings.

3.10 Effect of Load, Microhardness and Porosity on Wear Rate

Wear rates are calculated based on volume loss per unit of applied load as well as sliding distance. The variation of wear rate with load is shown in **Figure 10**. It is observed that the wear rate decreases with an increase in load for all coating systems examined in this investigation clearly suggesting that the depth of indentation is not a linear function of the applied load. At higher loads, the top coat of the sample is found to be removed with rapidity thus causing the bond coat to get exposed to abrasive disk. Once the bond coat starts experiencing the wear, greater amount of work hardening takes which again increases with the increase in the applied loads. At higher loads, work hardening effect shadows the effect of three body abrasion and converts it into an adhesive wear. Further, coefficient of friction is found to be slightly lower at 10, 15 N loads in comparison to 5 N load. When the applied loads are smaller, the contacts tend to bounce along the sliding surface causing the normal load to fluctuate. It is also found that the factors such as adhesion, work hardening and densification apart from the abrasive process influence the friction behaviour in steady state region.

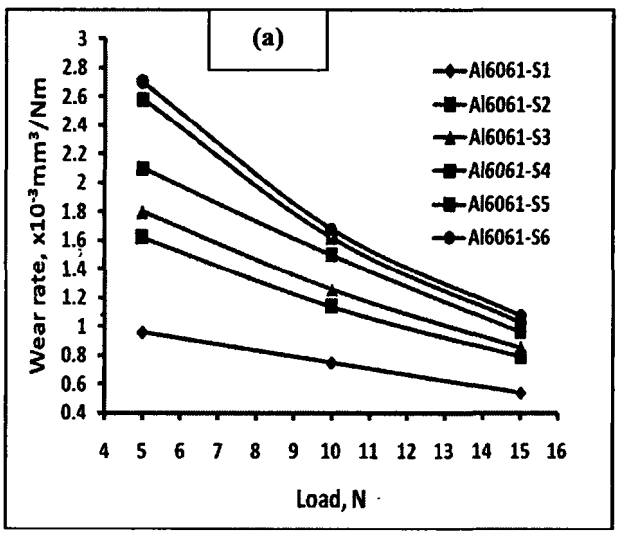

Fig. 10: Variation of Wear Rate with Load

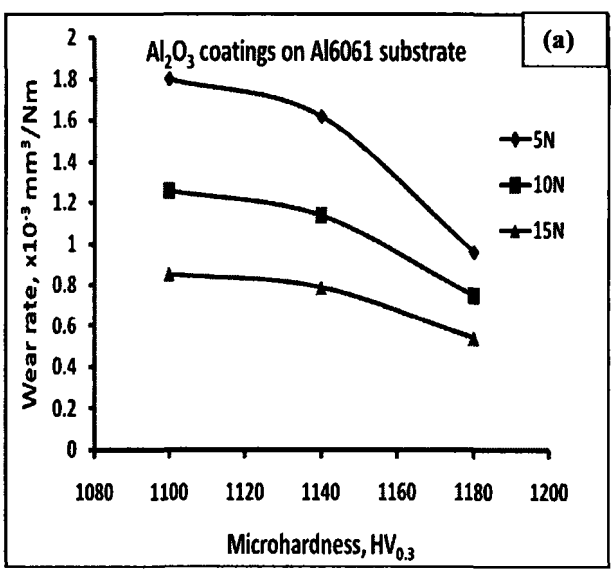

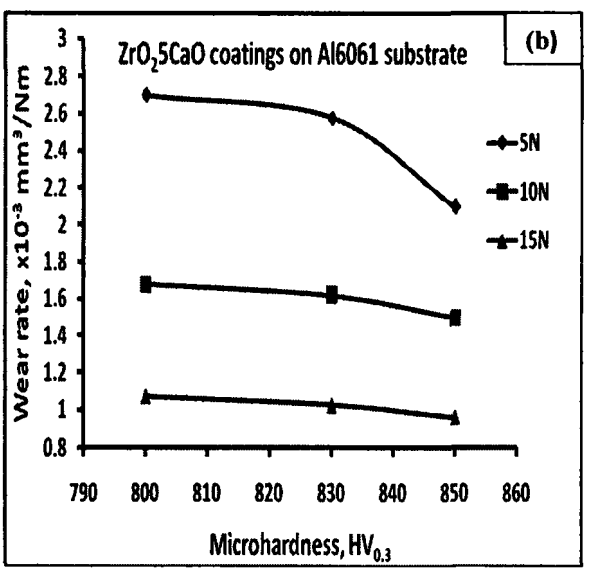

Fig. 11: Variation of Wear Rate of Coatings with Top Coat Microhardness (a) Alumina (b) ZrO_25CaO Coatings on Al6061 Substrate

It is generally found that the wear resistance of material is closely related to its micro hardness, toughness, coating defects and the ratio of its hardness to the hardness of the abrasive /35-39/. The graphs of wear rate versus microhardness (**Figure 11**) show that the wear rate increases with the decrease in micrhardness of the coating. It is evident that the microhardness of Al_2O_3 coatings is greater than that of ZrO_25CaO coatings. Also the wear loss of ZrO_25CaO coatings is higher than that of Al_2O_3 coatings. Thus wear rate is higher for coating with low hardness and vice versa. Similar trend is observed in the work of M. A. Moore et al. /40/. High hardness is desirable for obtaining improved wear resistance in case of both brittle and ductile materials while it improves further in case of brittle material with its improved toughness /37, 41/. Hardness has a significant effect on wear of materials by mechanisms of plastic deformation, while fracture toughness is a dominant factor during the process of wear involving brittle fracture /42/. In case of plasma sprayed coatings, better correlations are found between the hardness of the worn material and the wear modes where plastic deformation is a major mechanism /43/.

It is found that the wear rate of coating increases with coating porosity (Table 3) which is found to be due to either to inter-lamellar porosity or poor intersplat bonding in these coatings. The abrasion rate of bulk ceramic material is mainly dependent on the microstructural factors such as porosity. On the other, the microstructure of plasma sprayed ceramic coatings depends on the level of inter-lamellar bonding, including the horizontal crack density and shape factor and degree of flattening of the splats. It appears that these microstructural features which are unique to plasma sprayed coatings may have greater influence on their wear behavior than on their hardness.

4. CONCLUSIONS

In this study, two plasma sprayed oxide ceramic coatings, namely Al_2O_3 and ZrO_25CaO on Al-6061 substrate have been characterized in terms of microstructure, porosity, surface roughness, microhardness and wear properties. The experimental results led to the following conclusions

1. From the SEM cross-sections of coating systems it was observed that there is a variation in coating thickness by ±15 μm to ± 30μm from the actual value. It is mainly due to variation in speed of the plasma gun during spraying. This variation can be minimized by applying Robot Plasma Spraying technique.
2. From the Image Analyzer it was found that the porosity lies in the range of 5.5 to 8%. The porosity can be minimized by subjecting the coated components to laser treatment.
3. From the surface texture data, it was observed that the average roughness of alumina coatings varies from 3.5 to 5.5μm where as for ZrO_25CaO coatings, it varies from 4.5 to 7.2 μm.
4. The hardness of Al_2O_3 coatings varies from 1100 to 1190HV on Al-6061 and cast iron substrates where as the hardness of ZrO_25CaO coatings varies from 780 to 850 HV. The results show that hardness values lies in the standard range. By comparing hardness values it can be concluded that Al_2O_3 coating is harder than ZrO_25CaO coatings. It can be also concluded that microhardness decreases with increase in coating thickness and porosity.
5. From the wear test results it can be concluded that the predominant steady state mechanism of material removal was due to three body abrasion mechanism. The break-in-sliding coefficient was found to be more affected by load than by other test parameters. Friction coefficient increases with increase in load as well as with coating thickness. From the wear test results it is concluded that Al_2O_3 coatings withstand wear resistance more than ZrO_25CaO coatings. Finally it can be concluded that the pin-on-disk test can be used to understand certain relationships between the friction and wear behavior of thermally sprayed coatings. The results obtained showed that the wear test was able to discern the effects of the changes in the imposed test conditions. By proper control of test conditions and by selected changes of those conditions the physical wear mechanism involved in plasma sprayed coatings could be understood.

REFERENCES

1. B. Bhushan and B. K. Gupta, *Handbook of Tribology – Materials, Coatings and Surface Treatments,* McGraw-Hill, New York, (1991), p.168.
2. T.M. Yonushonic, *Thermal spray Technology,New Ideas and Processes,* ASM International, Metals Park, OH, (1989), p.239-243.
3. R.C. Novak, A.P.Matarese and R.P.Huston, *Thermal Spray Technology, New Ideas and Processes*, ASM International, Metals Park, OH (1989), p.273-281.
4. J.M. Guillemot, P.Dehaudt and M.Ducos, *Proc. 11th inter. Thermal Spraying Conference,* Pergamon Press, Newyark, (1986), p.513-521.
5. B.C. Inwood, Meyer, H.Grunow and P.E.Chandler, *Proc. 12th Thermal Spraying Conference, Vol. 1*, The Welding institute, Cambridge (1989), Paper 91.
6. L.M. Sheppard, *American Ceramic Society, Bull.***69**, p.1012(1990).
7. R.A. Miller, *EPRI Report*, AP-5078(1991).
8. A. Thomas Taylor, *Handbook of Thermal Spray Technology*, ASM International, Materials Park, OH, USA, p.171.
9. P.L. Ko and M. F.Robertson, *Wear*, **252**, p.880-893 (2002).
10. F. Rastegar and D. E. Richardson, *Surf. Coat. Technology*, **90**, p.156-193 (1997).
11. R.C. Tucker, *Int. J. of Powder Metallurgy*, **38**, p.45-53(2002).
12. R. Westergard, L. C.Erickson, N. Axen, H. M. Hawthrone and S. Hogmark, *Tribol. Int.* **31**, p.271-279 (1998).
13. D. Yoma, W. Brandl and G. Marginean, *Surface Coating Technol*, **138**, p.149-158(2001).
14. Y.Q. Fu, A.W.Batchelor, Y. Wang and K. A.Khor, *Wear*, **217**, p.132-139 (1998).
15. H. Liao, B. Normand and C.Coddet, *Surface Coat. Technol.* **124**, p.235-242(2000).
16. R.B. Heimann, *Key Engg. Materials*, **122/124**, p.399-442 (1996).
17. H. Herman, S. Sampath, K. H. Stern, *Metallurgical and ceramic protective coatings*, Chapman and Hall, London, (1996), p. 263.
18. G. Barbezat, A.R. Nicoll and A. Sickinger, *Wear,* **162/164,** p.529-537(1993).
19. V. Ramnath and N. Jayaraman, *Material Science Technol.*, **5**, p.382-388(1989).
20. J.E. Fernandez, R. Rodriguez, Y.Wang, R.Vijande and A.Rincon, *Wear,* **181-183,** p 417-425 (1995).
21. Roy Kamo, Dennis N. Assanis, Walter Bryzik, Thin Thermal Barrier Coatings for Engines, Transactions of SAE, Paper No. **890143**, p. 131-139 (1989).
22. V. Miyains, T. Matsuhisa and T. Ozawa, *Transactions of SAE*, Paper No. **890141**, p.117-129(1989).
23. Roy Kamo, *Transactions of SAE*, section-3, Paper No. **970204**, p.354-363(1997).
24. M. Vittal, J.A. Borek, *Transactions of ASME,* **121**, p. 218 (1999)
25. T. Hejwowski and A.Weronski, Vacuum, **65**, p.427 (2002).
26. R. Prasad, Ravindra and N.K. Samria., *Int. journal of mechanical sciences,* **31**, p.10 (1989).
27. Y. Xie and H.M. Hawthrone, *Wear*, **233/235**, p. 293-305(1999).
28. Y. Xie and H.M. Hawthrone, *Wear*, **225/235**, p.90-103(1999).
29. L.C. Erickson, H.M. Hawthrone and T. Troczynski, *Wear*, **250**, p.569-575(2001).
30. J.E. Fernandez, R. Rodriguez, Y. Wang, R. Vijende and A. Rincon, *Wear*, **181/183**, p. 417-425(1995).
31. O. Sarikaya, *Surf. Coat. & Technol.*, **190**, p.383-393(2005).
32. P.P. Psyllaki, M. Jeandin and D.I. Pantelis, *Materials Letters,* **47**, pp.77-82 (2000).
33. I.M. Kusoglu, E. Celik, H. Cetinel, I. Ozdemir, O. Demirkurt and K.Onel, *Surf. Coat. Technol.*, **200**, p.1173-1177(2005).
34. Giovanni Bolelli, Valeria Cannillo, Luca Lusvarghi and Tiziano Manfredini, *Wear*, **260**, p.1-18 (2006).
35. D. Tabor, *Wear-a critical synoptic view, Wear of Materials*, ASME, NY, (1977), pp 1-11.
36. S.J. Chu, H. Moon, B.J. Hockey and S.M. Hsu, *Acta Metall. Mater., 40*, p.185-192(1992).
37. S. Ramalingam and P.K. Wright, *J. Eng. Mater. Technol.*, **103**, p.151-156(1981).
38. M. Boas and M. Bamberger, *Wear*, **126**, p.197-210 (1988).

39. M.M. Kruchev, Principles of abrasive wear, *Wear*, **28**, p.69 (1974).
40. M.A. Moore and F.S. King, ,*Wear*, **60**, p.123-140(1980).
41. S.J. Cho, B.J. Hockey, B.R.Lawn, S.J. Bennison, *J. Am. Ceramic Society*, **72**, p.1249-1252 (1989).
42. I.M. Hutechings and Edward Arnold, *Friction and Wear of engineering materials*, Metallurgy and Material Science Series, 3rd Edition, England (1992).
43. L.C. Erickson, *Wear and microstructural integrity of ceramic plasma sprayed coatings*, Ph.D thesis, The University of British Columbia, (1999).